

# Studies on Structural and Magnetic Properties in Co/Sm Multilayers

Erwin

Department of Physics Faculty of Mathematics and Natural Sciences Riau University,  
Bina Widya Campus, Simpang Panam Km. 12.5, Pekanbaru 28293

Diterima 12-12-2009

Disetujui 08-05-2010

## ABSTRACT

Co/Sm multilayer films with structure of 20 [Co (x nm)/Sm (1.2 nm)] where  $x = 1.1, 2.2$  and  $4.2$  nm and 20[Co (4.2 nm)/Sm (x nm)] where  $x = 1.2$  nm to  $7.5$  nm were fabricated using dc magnetron sputtering. Each multilayer film consisted of 20 bilayers of Co layers with various thicknesses sandwiched with Sm layers. The application of low angle X-ray diffraction measurements to the characterization of these multilayers is described. The periodic layered structure with sharp interfaces was observed for all multilayer films. The measured magnetization values are lower than the values calculated in terms of the nominal concentration of cobalt in the multilayers. This implies significant "mixing" at small film thickness. The formation of a high magneto crystalline anisotropy of CoSm alloy at the interfaces, as a result of interdiffusion between Co and Sm layers was considered to be responsible for the increase of the coercivity for Co/Sm multilayer.

**Keywords:** coercivity, magnetic, microstructure, multilayer films, structure

## INTRODUCTION

In recent year, cobalt based alloys in the form of thin films and thin film multilayer structures consist of alternate magnetic and non magnetic layers of manometer thickness have attracted much attention due to their magnetic properties. One important application of such films is as high-density magnetic recording media. Many such alloys are based on the CoCr binary system with often multinary additions of such elements as Pt, Ta and B. An alternative binary system is that of CoRe alloys (Re- rare earth), and in particular the CoSm system. This allows, in principle and in equilibrium, the formation of a series of CoSm compounds with properties that reflect those of the compounds formed in bulk CoSm permanent magnets namely  $\text{Co}_{17}\text{Sm}_2$ ,  $\text{Co}_5\text{Sm}$  and  $\text{Co}_7\text{Sm}_2$ . There is also the additional interest in this system in that CoSm alloys can be deposited in the amorphous phase at Sm above about 20 atomic %.

According to (Murdock *et al.*, 1992), magnetic recording media for high-density magnetic data storage with low noise require a material consisting of small and magnetically isolated grains. In small grain sizes of about 10 nm or below, high magneto crystalline

anisotropy is needed in order to avoid thermal fluctuation that tends to destabilize the magnetization of the recorded bits (1997).

Early attempts to grow CoSm alloys in the form of thin films exhibiting large coercivity values were carried out by (Theuerer *et al.*, 1969; Gronou *et al.*, 1983), reported that CoSm films with high coercivity had been prepared by flash evaporation on glass substrates. They suggested that these films could be used as a high-density magnetic recording medium. Some recording experiments have been investigated, for example, by (Velu & Lambeth, 1992; Velu *et al.*, 1994). However, the growth characteristics of CoSm alloys including the concentration range (1982), the epitaxial relation between CoSm alloy films and underlayer materials, (1998; 1991), interaction effects (1998; 2000), and the magnetic switching volume (1995), suggest that improved magnetic properties of CoSm films could be obtained by utilization and optimisation of appropriate deposition conditions.

Several methods have been used in growing CoSm thin films. They include sputtering, evaporation and plasma spraying. Thin films with controlled geometry and surface smoothness as well as composition can be easily fabricated by the sputtering method (1991). It is commonly observed that sputter deposition of CoSm

thin films below 600°C usually produces alloys with an amorphous structure (1987). The amorphous structure of these alloys may limit their anisotropy and thus their coercivity. A higher value of coercivity can be simply achieved by introducing the crystalline state in the CoSm alloy by deposition with elevated substrate temperature or by post annealing of as-deposited films.

With regard to multilayer films, which are composed usually of ferromagnetic and non-magnetic thin layers, the interfacial mixing may exhibit novel magnetic properties. (1989; 1990) Work on multilayer films in which the nonmagnetic layer is composed of a rare earth and metalloid elements has been carried out for ferromagnetic materials forming the ferromagnetic layers. It was reported by Petford-Long *et al.*, (1990) that interfacial mixing exists for the Co/W structure that affects the magnetic properties.

This paper is concerned with the investigation of magnetic and structural properties of Co/Sm multilayer films. This study is driven by fundamental interest and by the need to design materials with magnetic properties which might be suited for high density magnetic recording media. Multilayer films of alternatively deposited ferromagnetic and nonmagnetic layers are also proving to be important for understanding the fundamental physics of interacting magnetic films.

## MATERIALS AND METHODS

The Co/Sm multilayer films were deposited onto Si (100) substrates by dc magnetron sputtering with a sputtering pressure of  $4 \times 10^{-8}$  mbar of argon gas and the deposition rates were about 0.21 nm/s and 0.31 nm/s for Co and Sm respectively. The samples were divided into two groups. The first group of samples takes the form of 20[Co (x nm)/Sm (1.2 nm)]. Each multilayer film consisted of 20 bilayers of Co layers with various thicknesses sandwiched with Sm layers of 1.2 nm thick. The second group of multilayer films has the form of 20[Co (4.2 nm)/Sm (x nm)] in which the samples have the same Co layer thickness of 4.2 nm and the Sm layer thickness is progressively increased from 1.2 nm to 7.5 nm. Again, each multilayer film consists of 20 bilayers of 4.2 nm of Co layers sandwiched with Sm of various thicknesses.

The periodic structure i.e., sharp interfaces, in the samples of the samples was studied by small angle X-ray diffraction. The data obtained were processed with special computer program which is called XREALM

software (1988). Layer thicknesses were determined by sputtering rate and from the low angle X-ray diffraction patterns. The magnetic properties of the samples were studied by alternating gradient force magnetometer (AGFM) and vibration sample magnetometer (VSM). High-resolution transmission electron microscopy (HRTEM) has been used to analyse the microstructure of some of the as-deposited samples.

## RESULT AND DISCUSSION

Low Angle X-Ray Diffraction Profiles. The low angle x-ray diffraction technique was used to investigate the structure of Co/Sm multilayer films. Figure 1 shows the low angle diffraction patterns for multilayer films with structure of 20[Co(x nm)/Sm(1.2 nm)] where  $x = 1.1, 2.2, \text{ and } 4.2$ . Computer simulations of the data, perform using XREALM softwar (1988) for multilayer films are included for comparison. In the simulated reflectivity profile, variables such as the layer thickness of the Co and Sm films, the roughness of the substrate and the layers, and the relative densities of substrate and films, can be adjusted so that one can obtain the closest fit to the experimental data. It can be seen that almost all the reflection peak positions of the multilayer films correspond to those in the simulated reflectivity profile. From the simulated reflectivity profile analysis, for example, the multilayer film with  $x=1.1$  nm, it was found that the thickness of periodic bilayer was 2.22 nm, which corresponds to the thickness of Co and Sm layers of 1.10 nm and 1.12 nm respectively.

From Figure 1, the multilayer films show several orders of diffraction peaks, indicating the periodic nature of the sample. For the multilayer film with  $x = 1.1$  nm, finite size oscillations (Kiessig fringes) persist to 5.5 degrees, implying that the overall surface of the multilayer film is smooth. However, for  $x = 2.2, \text{ and } 4.2$  nm finite size oscillations are not very clear, suggesting that the surface of the films is not smooth. With increasing Co layer thickness, diffraction peaks shift to a smaller value of angle of incidence suggesting that the bilayer thickness is increased. From the position of low angle XRD peaks shown in Figure 1, the thickness of the periodic layer (bilayer) for all samples could be calculated. Table 1 shows the bilayer thickness for nominal, simulated and calculated (low angle XRD).

Magnetic Properties Figure 2 shows hysteresis loops measured at room temperature for multilayer films

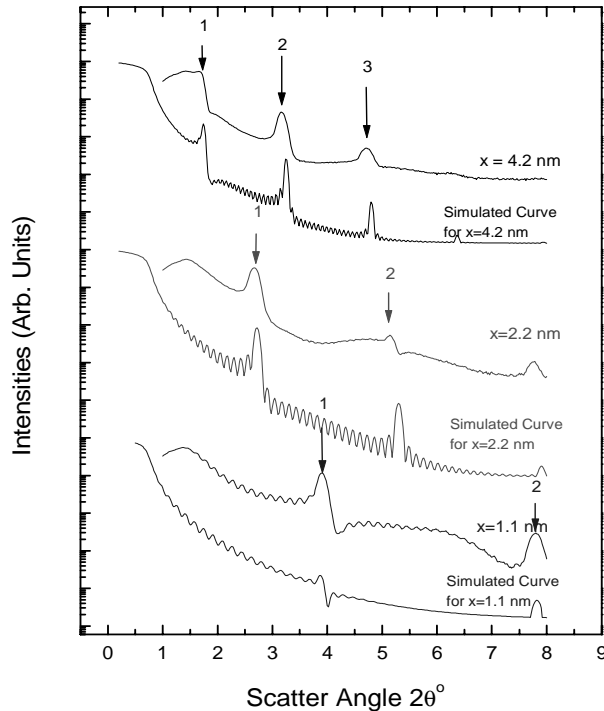


Figure 1. Low angle x-ray reflectivity profiles of multilayer films with structure of 20[Co (x nm)/Sm (1.2 nm)]. The order of the Bragg peaks is marked on some curves.

Table 1. Bilayer thickness of Co/Sm multilayer films with structure of 20[Co (x nm)/Sm (1.2 nm)].

Sample Code	Bilayer Thickness ( nm )		
	Nominal	Simulated Results	Low Angle XRD Results
ML10A	2.3	2.2	2.20 ± 0.01
ML10B	3.3	3.3	3.30 ± 0.16
ML10C	4.2	4.2	4.20 ± 0.23
ML10D	5.4	5.4	5.40 ± 0.47

with the structure of 20[Co (x nm)/Sm (1.2 nm)] for  $x=1.1, 2.2$  and  $4.2$  nm. For the multilayer film with Co layer thickness of  $1.1$  nm, the coercivity is about  $740$  Oe. The hysteresis loop which has low remanence magnetization ratio (around  $0.6$ ) exhibits a small kink in both field directions i.e., at near zero field indicating the presence of either a second magnetically soft phase or low field nucleation phenomena that initiate magnetization reversal (1997). The large value of coercivity of this multilayer film compared to those with thicker Co layers is interpreted as being due to possible interlayer mixing at a composition of about  $3:1$  (equivalent to the  $\text{Co}_3\text{Sm}$  phase). The saturation magnetization value for this multilayer film is about  $150$   $\text{emu}/\text{cm}^3$ , which is similar to that for the  $\text{Co}_3\text{Sm}$  compound, hence the choice of  $\text{Co}_3\text{Sm}$  as the 'mixing' composition.

The effect of a greater Co layer thickness on the loop for Co layer thickness of  $2.2$  nm is shown in Figure 2b. The coercivity of this multilayer decreases

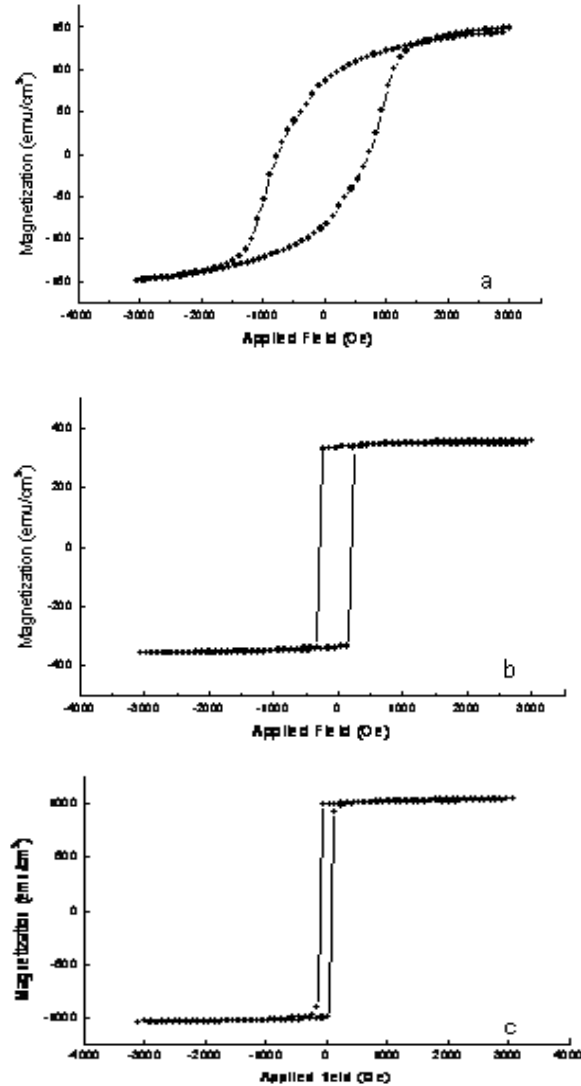


Figure 2. Hysteresis loop measured at room temperature for multilayer films with structure of 20[Co (x nm)/Sm (1.2 nm)], where (a)  $x = 1.1$  nm, (b)  $x = 2.2$  nm, and (c)  $x = 4.2$  nm.

very significantly to  $230$  Oe with a higher loop squareness ( $0.95$ ). The saturation magnetization value for this multilayer film is about  $350$   $\text{emu}/\text{cm}^3$ . Increasing the Co layer thickness further ( $4.2$  nm) leads to a further decrease in coercivity ( $90$  Oe). The magnetization value increased to about  $1020$   $\text{emu}/\text{cm}^3$ . The hysteresis loop exhibits a higher squareness ( $0.97$ ) as shown in Figure 2c. An increase of magnetization value with increasing Co layer thickness is reasonable, and is due to an increase in the amount of the magnetic Co in the multilayer. However, the measured magnetization values are lower than the values calculated in terms of the nominal concentration of cobalt in the multilayers. This is particularly so for the smaller values of  $x$ , i.e., for  $x=1.1$  nm. The calculated magnetization of about  $670$   $\text{emu}/\text{cm}^3$  compares to the measured value of  $150$   $\text{emu}/\text{cm}^3$ . The respective values for  $x=2.2$  nm are  $900$   $\text{emu}/\text{cm}^3$ .

$\text{cm}^3$  and  $350 \text{ emu/cm}^3$  and for  $x=4.2 \text{ nm}$  are  $1090 \text{ emu/cm}^3$  and  $1020 \text{ emu/cm}^3$ . This implies significant mixing at small film thickness.

The interaction effect given by  $\delta M$  for the three multilayers is shown in Figure 3. For the multilayer film with  $x = 1.1 \text{ nm}$  the  $\delta M$  shows a broad positive and then negative peak. This could be due to exchange coupling over an extended field range between the Co layers, but there is also a strong dipolar coupling which becomes obvious at larger fields and moderates the exchange coupling because the Co layers are close enough for significant magnetostatic dipolar coupling.

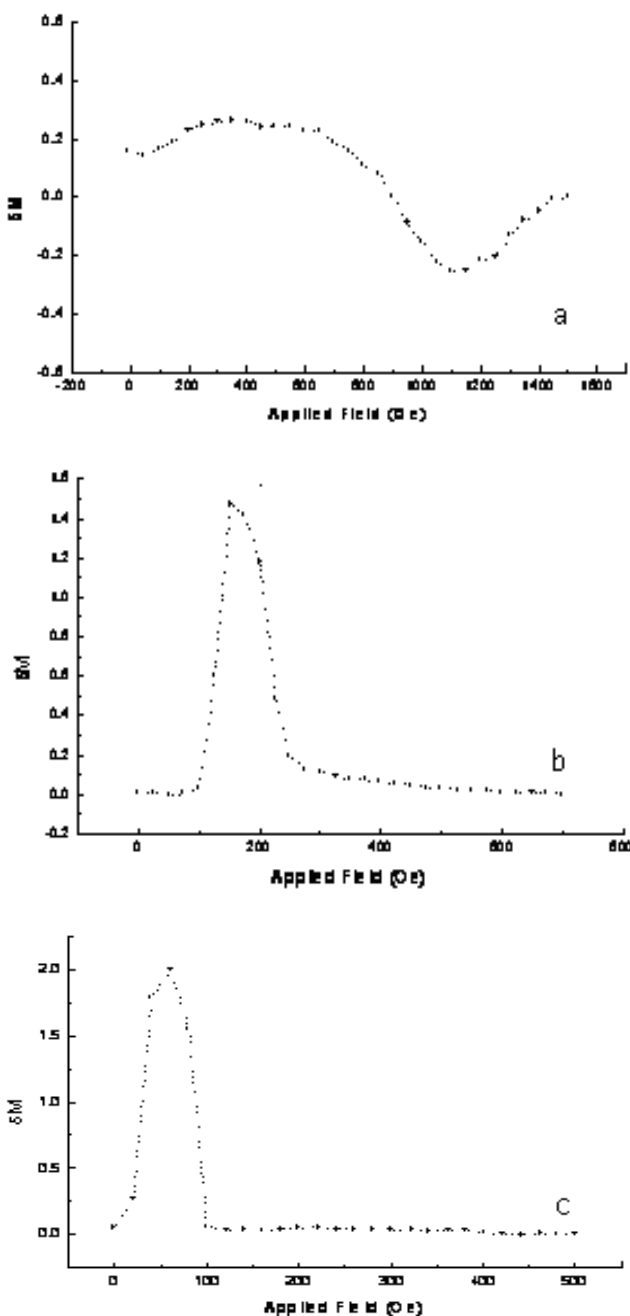


Figure 3.  $\delta M$  curves as a function of applied field for multilayer films with structure of  $[20x(\text{Co } x \text{ nm}/\text{Sm } 1.2 \text{ nm})]$  (a)  $x = 1.1 \text{ nm}$  (b)  $x = 2.2 \text{ nm}$  and (c)  $x = 4.2 \text{ nm}$ .

The boardening of the positive  $\delta M$  is due to the interlayer dipolar coupling in the multilayer film, which prevents any sharp cooperative reversal (2001). This result is consistent with the lower loop squareness, Figure 2(a).

For multilayer films with  $x = 2.2$  and  $4.2 \text{ nm}$  the interaction effect ( $\delta M$ ) shows a very sharp positive peak. The narrow positive peak of  $\delta M$  is indicative of stronger exchange coupling in the Co layers and possibly between the Co layers. This strong coupling dominates any dipolar coupling that is present. The exchange coupling is even stronger for the thickest Co layers, as shown in Figure 3(c). This result is consistent with higher loop squarenesses, Figure 2(b) and (c). It is difficult to assess the effect of interface roughness at the larger values of  $x$  on the magnetic interactions in the films but any correlated or uncorrelated roughness would have some effect through the Néel-type mechanism/orange PEEL COUPLING (1962).

**Microstructural Properties.** A high-resolution transmission electron microscopy (HRTEM) cross-sectional image of a multilayer film with structure of  $20[\text{Co}(1.1 \text{ nm})/\text{Sm}(1.2 \text{ nm})]$  is shown in Figure 4. The sharp periodic layers of Co and Sm can be clearly distinguished as a result of the difference in electron scattering of the sample. The darker Co layers are clearly separated from the brighter Sm layers. A regular periodicity without discontinuity of the bilayers structure can be clearly seen, especially close to the substrate. Another feature that can be noticed from Figure 4 is that the roughness of the layers increases with distance from the substrate. The bilayer thickness derived from the cross-sectional HRTEM images of the multilayer films is in good agreement with the one obtained from the low angle X-ray diffraction measurement shown in Figure 1. The thicknesses of the Co and Sm layers



Figure 4. High resolution transmission electron microscopy (HRTEM) cross sectional image of multilayer films with structure of  $20[\text{Co}(1.1 \text{ nm})/\text{Sm}(1.2 \text{ nm})]$

given by Figure 4 are also well agree with the nominal deposition values.

Figure 5 shows a highly magnified micrograph of this multilayer film. Within the Co layers some crystalline grains are observed. These crystalline grains are a few nanometres (1-2 nm) in size (nanocrystallites) while the Sm layers appear to be amorphous. The diffuse structure of the Sm layers and the interfaces is especially obvious towards the top of the micrograph and away from the substrate.

**The Effect of Sm Layer Thickness.** Low Angle X-ray Diffraction Profiles. Figure 6 shows a set of low angle x-ray diffraction patterns for multilayer films with a structure of 20[Co (4.2 nm)/Sm (x nm)] where x ranges from 1.2 to 7.5 nm. Computer simulation of the data for x=1.2 nm is included for comparison. From the figure,

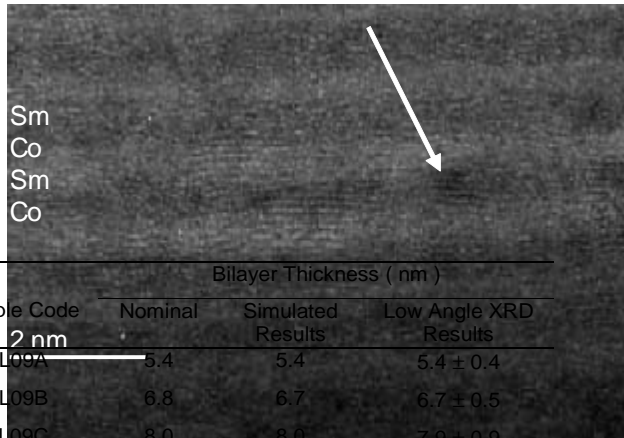


Figure 5. Large magnification of HRTEM cross-sectional image of multilayer films with structure of 20[Co (1.1 nm)/Sm (x nm)]. Arrows indicate nanocrystals.

Sample Code	Bilayer Thickness ( nm )		
	Nominal	Simulated Results	Low Angle XRD Results
ML09A	5.4	5.4	5.4 ± 0.4
ML09B	6.8	6.7	6.7 ± 0.5
ML09C	8.0	8.0	7.9 ± 0.9
ML09D	9.6	8.9	8.8 ± 0.8
ML09E	11.0	10.5	10.5 ± 0.5
ML09F	11.7	11.2	10.9 ± 1.7

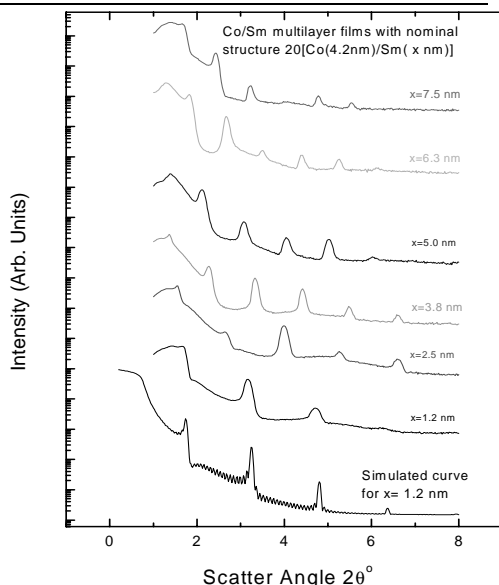


Figure 6. Low angle x-ray diffraction profiles of multilayers of 20[Co(4.2 nm)/Sm (x nm)], where x ranges from 1.2 to 7.5 nm.

Bragg maxima are clearly observed even at relatively high diffraction angles, suggesting the periodic nature of the samples. For all the multilayer films the interface (Kiessig) fringes from the top and bottom surfaces of the multilayer film stack are not very clear, suggesting that these surfaces are less well-defined. With increasing Sm layer thickness, diffraction peaks shift to a smaller value of angle of incidence suggesting that the bilayer thickness is increased. From the position of low angle XRD peaks shown in Figure 6, the thickness of the periodic layer (bilayer) for all samples could be calculated. The nominal value of the Co and Sm layer thicknesses was estimated based on the deposition rates of Co and Sm.

From the simulated reflectivity pattern analysis, it was found, as an example, that the thickness of a periodic bilayer was 8 nm, which corresponds to the thickness of Co and Sm layers of 4.2 nm and 3.8 nm respectively. From low angle XRD measurement, it was found that the thickness of that periodic bilayer was estimated from the position of Bragg peaks as about 7.9 nm. Table 2 shows in comparison the excellent agreement between nominal, simulated and experimental bilayer thickness of the multilayers. However, it can be seen that at higher bilayer thicknesses the experimental and simulated values fall below the nominal value due to interface roughness or mixing.

**Magnetic Properties.** Figure 7 shows the saturation magnetization values of the 20 [Co (4.2 nm)/Sm (x nm)] multilayers where x ranges from 1.2 to 7.5 nm. The theoretical values are included for comparison. Measurements of the saturation magnetization at room temperature show that the magnetization per unit volume of the multilayer films decreases when the Sm layer thickness is increased. This result reflects the fact that higher Sm layer thickness will increase the amount of nonmagnetic element Sm in the multilayer thus lowering its magnetization. Compared to theoretical values, it is

Table 2. Bilayer thickness of Co/Sm multilayer films with structure of 20[Co (4.2 nm)/Sm (x nm)].

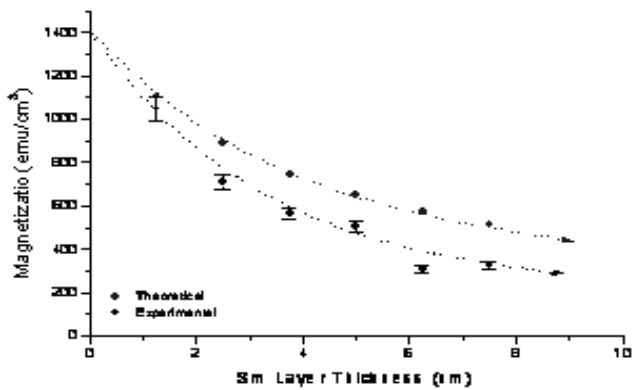


Figure 7. Magnetization of 20[Co (4.2 nm)/Sm (x nm)] multilayers as a function of Sm layer thickness; the red line represents theoretical values calculated from equation (2).

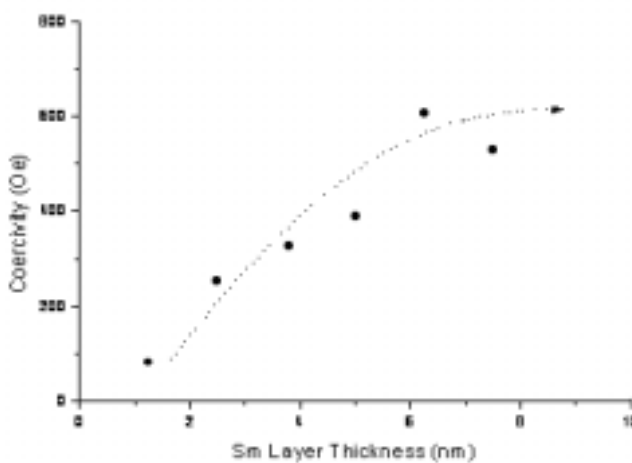


Figure 8. Coercivity of Co/Sm multilayer films with nominal structure of 20[Co (4.2 nm)/Sm (x nm)], where x ranges from 1.2 to 7.5 nm.

obvious that the measured saturation magnetization exhibits lower values. This result may be ascribed to the intermixing of Co and Sm layers in the formation of a thin magnetic or nonmagnetic CoSm 'alloy'.

Figure 8 is a plot of the coercivity of these multilayer films as a function of Sm layer thickness. It can be seen that the coercivities of the multilayer films increases when Sm layer thicknesses increase. The increase in coercivity with increasing samarium layer thickness can be interpreted as being due to surface roughness or mixing, which increases when the Sm layer thickness is increased. This phenomenon leads to the formation a  $\text{Co}_{100-x}\text{Sm}_x$  alloy at the interface between Co and Sm layers. This effect is supported by the results shown in the low angle XRD measurement shown in Figure 6 in which the diffraction peaks become slightly broader as Sm layer thickness is increased. It also mirrors the coercivity behaviour in Figure 8 where a relative preponderance of cobalt leads to lower coercivities.

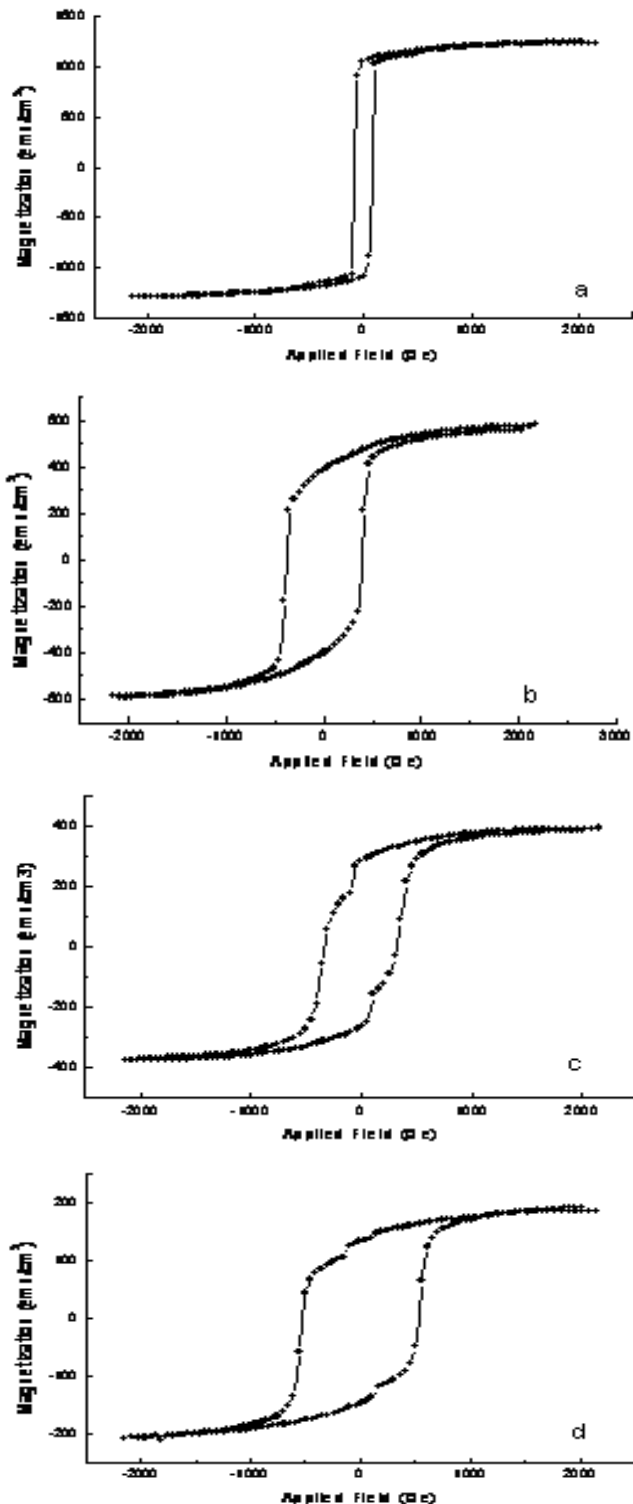


Figure 9. Hysteresis loops at room temperature for multilayer of 20[Co(4.2 nm)/Sm (x nm)] with (a)  $x=1.2$ , (b)  $x=3.8$ , (c)  $x=5.0$  and (d)  $x=7.5$

Figure 9 shows typical hysteresis loops measured at room temperature for as-deposited multilayer films. As the Sm layer thickness is increased the shape of the hysteresis loop changes from high (square-like) to low loop squareness. The hysteresis loop of the multilayer films with Sm layer thickness of 1.2 nm is nearly square with a coercivity of 84 Oe. Above this

thickness, the hysteresis loops becomes progressively less square. For the multilayer film with Sm layer thickness of 5.0 nm the hysteresis loop exhibits a small kink in both field directions, i.e., at near zero field. When the Sm layer thickness is increased further to 7.5 nm, again the hysteresis loop shows a small kink near zero field indicating that the magnetic layers are well separated and non-coherent rotation or the presence of a second phase is certainly established.

**Microstructural Properties.** Figure 10 shows a cross-sectional image of the multilayer film 20[Co(4.2nm)/Sm(3.8nm)], along with the corresponding diffraction pattern. The periodic Co and Sm layers are clearly seen in this image. The apparent bilayer thickness of the Co and Sm estimated from the HRTEM micrograph is less than the nominal value of 4.2 nm and 3.8 nm of Co and Sm respectively. This is due to some interdiffusion between Co and Sm layers as discussed above. The thicker, darker layer is the Co layer while the thinner, brighter layer is the Sm layer.

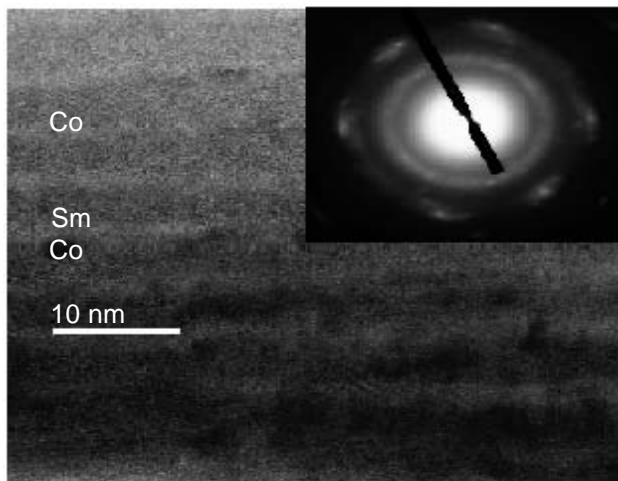


Figure 10. Cross-sectional electron micrograph of a 20[Co(4.2nm)/Sm(3.8nm)] multilayer film.

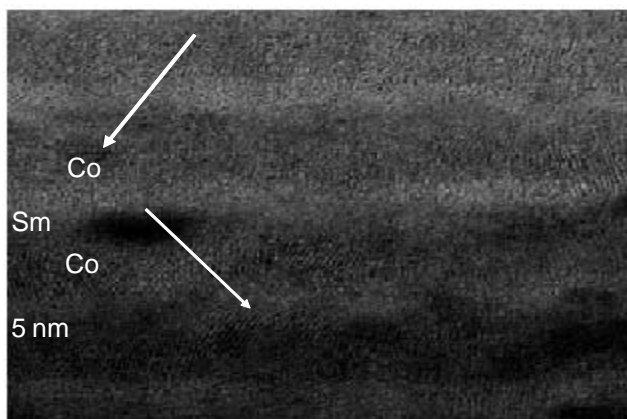


Figure 11. Large magnification HRTEM cross-sectional image of multilayer films with structure of 20[Co ( 4.2 nm)/Sm (3.8 nm)]. Arrows indicate nanocrystals.

Another feature that can be noticed from this picture is the long “waviness” of the layers which decreases further away from the substrate, indicating that the flatness of the layers is also increasing but the sharpness of the interfaces becomes less defined with distance from the substrate. The electron diffraction pattern (inserted in Figure 10) from this multilayer film reveals two broad rings associated with an amorphous structure. The first diffuse ring comes from Sm spacings, which can be clearly seen in the electron diffraction pattern of a planar sample (Figure 10). The second broad ring exhibits faint arc shaped reflections indicating some texture in the cobalt component of the multilayer.

Figure 11 shows a highly magnified micrograph of this multilayer film. The brighter Sm rich layer has a thickness that is smaller than its nominal thickness (3.8 nm). The Co layers contain 3-6 nm size nanocrystals with similar lattice fringes as indicated by arrows while the Sm layers appears to be amorphous as can be clearly seen. Obviously, the size of nanocrystallites has increased for thicker Co layers compared to multilayer with lower Co layer thickness, as shown in the HRTEM micrograph Figure 5.

## CONCLUSION

Multilayer films of Co/Sm were investigated in order to explore their intrinsic properties and to modify their magnetic properties via interdiffusion between the Co and Sm layers. The study revealed that an increase in the Co layer thickness lead to a large decrease in the coercivity with an accompanying increase in the saturation magnetization. This behaviour was attributed to an increase in the amount of the magnetic Co in the multilayer. The  $dM$  studies showed that the exchange interaction among the grains in the layers is stronger for thicker Co layers and results in significant reduction of the coercivity of the multilayers. However, for thinner Co layers the  $dM$  shows both broad positive and negative peaks. This could be due to exchange coupling between the Co layers but there is also strong dipolar coupling which moderates the exchange coupling and becomes obvious at large fields. This behaviour was interpreted as being due to the separation of the Co layers that is close enough for significant magnetostatic dipolar coupling. The multilayer structure observed by electron microscopy (HRTEM) revealed a well-defined layer structure. Low angle X-ray diffraction profiles supported these results through well-defined Bragg peaks although

Kiessig fringe are not always very clear. The variation of Sm layer thickness revealed that an increase in the Sm thickness lead to an increase in the coercivity, accompanied by a decrease in the saturation magnetization. The enhancement of coercivity can be interpreted as being due to an increase in the roughness and mixing of the layers.

### ACKNOWLEDGMENTS

The author would like to thank Philip J. Grundy of the University of Salford, Manchester UK for performing the sputtering and experiments.

### REFERENCES

- Antel Jr, W.J., Laidler, H. & Marrows, C.H.** 2001. Interaction effects in disordered multilayers. *J. Appl. Phys* **89**: 7071-7073.
- Benaissa, M. & Krishnan, K.M.** 1998. Magnetic anisotropy and its microstructural origin in epitaxially grown SmCo thin films. *IEEE Tans. Magn* **34**: 1204-1206.
- Cadieu, F.J., Cheng, T.D., Wickramasekara, L. Kamprath, N., Hedge, H. & Liu, N.C.** 1987. The magnetic properties of high iHc SmCo, NdFeB, and SmTiFe films crystallized from amorphous deposits. *J. Appl. Phys* **62**: 3866-3872.
- Charap, S.H., Lu, P.L. & He, Y.** 1997. Thermal stability of recorded information at high densities, *IEEE Trans. Magn* **33**: 978-983.
- Cui, F.Z. Fan, Y.D., Wang, Y., Vredenberg, A.M., Draaisma, H.J.D. & Xu, R.** 1990. A new magnetic multilayer system: Iron bismuth. *J. Appl. Phys* **68**: 701-704.
- Geiss, V., Kneller, E. & Nest, A.** 1982. Magnetic behavior of amorphous Sm-Co Alloy film. *J. Appl. Phys* **A27**: 79-88.
- Gronou, M. Goeke, H., Schuffler, D. & Sprenger, S.** 1983. Correlation between domain wall properties and material parameters in amorphous SmCo-films. *IEEE Trans, Magn* **19**: 1653-1655.
- Majeticch, S.A., Chowdary, K.M. & Kirkpatrick, E.M.** 1998. Size and interaction effects in the magnetization reversal in SmCo5 nanoparticles. *IEEE Trans. Magn* **34**: 985-988.
- Murdock, E.S., Simon, R. & Davidson, R.** 1992. Roadmap for 10Gbit/in<sup>2</sup> Media Challenges, Paper JA-01, Intermag '92, St. Louis, Missouri USA.
- Petford-Long, K.A., Grundy, P.J. & Jakubovics, J.P.** 1990. Structure and magnetic properties of Co based multilayers. *IEEE Trans. Magn* **26**: 2733-2735.
- Robert, P.** 1991. *'Thin Film Process II'*, Edited by J.L. Vossen and W. Kern, Academic Press, Inc, pp 177.
- Romero, S.A., Cornejo, D.R., Rhen, F.M., Neiva, A.C., Tabacniks, M.H. & Missell, F.P.** 2000. Magnetic properties and underlayer thickness in SmCo/Cr films. *J. Appl. Phys* **87**: 6965-6967.
- Singleton, E.W., Shan, Z.S., Jeong, Y.S. & Sellmyer, D.J.** 1995. Magnetic switching volumes of CoSm thin film for high density longitudinal recording. *IEEE Trans. Magn* **31**: 2743-2745.
- Stearns, M.B., Lee, C.H. & Groy, T.L.** 1989. Structural studies of Co/Cr multilayered thin film. *Phys. Rev* **B40**: 8256-8269.
- Theuerer, H.C., Nesbitt, E.A. & Bacon, D.D.** 1969. High Coercive Force Rare Earth Alloy Films by Getter Sputtering. *J. Appl. Phys* **40**: 2994-2996.
- Velu, E.M.T. & Lambeth, D.N.** 1992. High density recording on SmCo/Cr thin film media. *IEEE Trans. Magn* **28**: 3249-3251.
- Velu, E.M.T. & Lambeth, D.N.** 1991. CoSm based high coercivity thin films for longitudinal recording. *J. Appl. Phys* **69**: 5175-5177.
- Velu, E.M.T., Lambeth, D.N., Thornton, J.T. & Russel, P.E.** 1994. AFM structure and media noise of CoSm/Cr thin films and hard disk. *J. Appl. Phys* **75**: 6132-6134.
- Yan, M.L., Shan, Z.S., Liu, Y. & Sellmyer, D.J.** 1997. High coercivity SmFeAlC thin films fabricated by multilayer sputtering. *IEEE Trans. Magn* **33**: 3706-3708.